Original Article

Author for correspondence:
R. C. Chamberlain, MD, Department of Pediatrics, Division of Pediatric Cardiology, Duke University Hospital, DUMC Box 3090, Durham, NC 27710, USA. Tel: +1 919 681 6340; E-mail: reid.chamberlain@duke.edu

CAMBRIDGE
UNIVERSITY PRESS

Estimating radiation exposure during paediatric cardiac catheterisation: a potential for radiation reduction with air gap technique

Reid C. Chamberlain[1] , Alexis C. Shindhelm[2], Chu Wang[3], Gregory A. Fleming[1] and Kevin D. Hill[1]

[1]Department of Pediatrics, Duke University Medical Center, Durham, NC, USA; [2]Department of Bioengineering, Duke University Pratt School of Engineering, Durham, NC, USA and [3]University of Pittsburgh, Radiation Safety Office, Pittsburgh, PA, USA

Abstract

Introduction: The air gap technique (AGT) is an approach to radiation dose optimisation during fluoroscopy where an "air gap" is used in place of an anti-scatter grid to reduce scatter irradiation. The AGT is effective in adults but remains largely untested in children. Effects are expected to vary depending on patient size and the amount of scatter irradiation produced. *Methods:* Fluoroscopy and cineangiography were performed using a Phillips Allura Fluoroscope on tissue simulation anthropomorphic phantoms representing a neonate, 5-year-old, and teenager. Monte Carlo simulations were then used to estimate effective radiation dose first using a standard recommended imaging approach and then repeated using the AGT. Objective image quality assessments were performed using an image quality phantom. *Results:* Effective radiation doses for the neonate and 5-year-old phantom increased consistently (2–92%) when the AGT was used compared to the standard recommended imaging approaches in which the anti-scatter grid is removed at baseline. In the teenage phantom, the AGT reduced effective doses by 5–59%, with greater dose reductions for imaging across the greater thoracic dimension of lateral projection. The AGT increased geometric magnification but with no detectable change in image blur or contrast differentiation. *Conclusions:* The AGT is an effective approach for dose reduction in larger patients, particularly for lateral imaging. Compared to the current dose optimisation guidelines, the technique may be harmful in smaller children where scatter irradiation is minimal.

In patients with congenital heart disease (CHD) and acquired heart disease, cardiac catheterisation remains a significant source of low-dose ionising radiation.[1] Low-dose ionising radiation exposure causes DNA damage; and epidemiological studies link radiation exposure to an increased risk of both leukaemia and solid tumours.[2]

Recognising the potential for significant risks associated with exposure to low-dose ionising radiation, current guidelines endorse optimisation of imaging parameters during cardiac catheterisation.[3] One approach for dose optimisation is the air gap technique (AGT). The AGT consists of three key features: (1) removing the anti-scatter grid, (2) raising the camera height allowing the resulting air gap to reduce scatter irradiation to the image detector while also increasing geometric magnification, and (3) reducing the fluoroscopic magnification setting to offset the geometric magnification (Fig 1). Both the removal of the anti-scatter grid and reduction in fluoroscopic magnification settings reduce the delivered doses; however, these dose gains may be offset by raising the camera height, which causes fluoroscope auto-exposure controls to increase the delivered dose. Moreover, current recommendations advise against the use of an anti-scatter grid in children < 20 kg because smaller children produce less scatter irradiation.[3] Thus, the net effect of the AGT on the delivered dose varies depending on the amount of scatter irradiation, the relative dose changes associated with changes in magnification, and the relative difference in camera height. All of these factors are directly related to the volume of tissue that the X-ray beam must traverse and therefore the size of the patient and the beam angle. The AGT has been shown to reduce radiation doses during adult cardiac catheterisation and interventional radiology procedures.[4–6] Although some paediatric catheterisation laboratories have adopted the practice,[7] the AGT has not been tested across the range of sizes of patients undergoing paediatric cardiac catheterisation. Thus, it remains unclear as to when the net effect is beneficial or harmful for anterior–posterior and lateral fluoroscopy.[8]

In our study, we sought to compare radiation dosing and effective dose estimations between standard recommended imaging techniques and the AGT in paediatric cardiac catheterisation. Due to increased scatter irradiation in larger patients, we hypothesise AGT would have differential effects on absorbed radiation, with the greatest benefit in larger patients. Furthermore, we
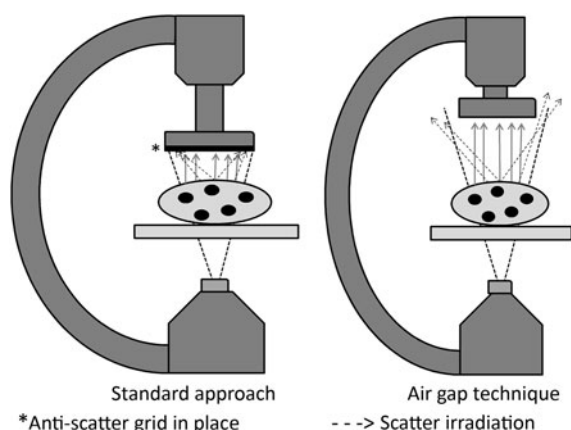
Figure 1. Schematic comparing the air gap technique to standard imaging.

hypothesised that geometric magnification from the AGT would have minimal effect on image blur when compared to standard imaging.

Materials and methods

Dosimetry verification phantoms and imaging protocol

Three ATOM dosimetry anthropomorphic phantoms (CIRS, Norfolk, Virginia, United States of America) representing a neonate (51 cm, 3.5 kg, thorax dimension 9×10.5 cm^2), a 5-year-old child (110 cm, 19 kg, thorax dimension 14×17 cm^2), and a teenage female (160 cm, 55 kg, thorax dimension 20×25 cm^2) were used for imaging simulation and radiation dose estimation. The dosimetry phantoms are manufactured using tissue equivalent epoxy resins with linear attenuation within 1% for bone and soft tissue and within 3% for lung tissue at photon energies from 30 keV to 20 MeV. Imaging was performed using a Philips Allura XP FD 10/10 (Philips Healthcare, Amsterdam, the Netherlands) biplane fluoroscopy system with a 70-line anti-scatter grid. The dosimetry phantoms were placed in the centre of the fluoroscopy table with imaging field of views and camera positioning adjusted by a trained paediatric interventional cardiologist to approximate typical imaging per the standard operating technique. This procedure was repeated with AGT. The protocol for the standard operating technique involves minimised source-to-image distances of 93 cm for anterior–posterior and 113 cm for lateral projections. Imaging was performed following the guideline recommendations, with the anti-scatter grid removed for patients <20 kg.[3] The protocol for AGT, performed with the anti-scatter grid removed, was with source-to-image distances increased by 20–113 cm for anterior–posterior projections and by 16–129 cm for lateral projections. In the lateral projection, a source-to-image distance increase of 20 cm, identical to the anterior–posterior projection, resulted in disproportionately greater geometric magnification compared to standard imaging. Therefore, in the lateral projection a 16-cm increase in source-to-image distance was used to reconstitute a more comparable image to standard operating technique. Periphery collimation on all sides was 1 inch for standard operating technique and adjusted as needed to provide a replicate image with AGT. No peripheral filters were used. Field-of-view magnification varied based on dosimetry phantom size and technique. For the neonate, anterior–posterior magnification was 6, 8, and 10 inches with lateral magnification of 6 and 8 inches. For the 5-year-old, anterior–

posterior and lateral magnification was 8 and 10 inches. For the teenager, anterior–posterior and lateral magnification was 10 inches. Fluoroscopy pulse rates were set at 15 pulses/second and cineangiography was obtained at 15 frames/second at a pulse width of 0.4 ms. Filtration was constant and consistent with the institution's current clinical parameter of 0.4 mm of copper and 1 mm of aluminium. The Bucky factor for our fluoroscope's anti-scatter grid, representing the ratio of air Kerma (mGy) with and without the anti-scatter grid, was tested with all other imaging parameters held constant and found to range from 1.5 to 1.8 depending on the phantom size. Beam parameters, including peak kilovoltage (kVP) and milliampere (mA), were allowed to vary based on the fluoroscope's automatic exposure controls to maintain image quality, consistent with the standard imaging protocols. All imaging was performed for 5–10 s of continuous fluoroscopy and cineangiography, respectively, then repeated in sequence to assess the impact of each individual parameter manipulation while holding all other imaging parameters constant. For each imaging sequence, radiation-related output values from the fluoroscopy unit were recorded, including beam parameters in kVP, mA, air Kerma in mGy and dose area product (DAP). To account for any variation in exposure time, the reported values were standardised per 1000 frames.

Effective dose estimations

Given the significant variation in paediatric patient size, effective radiation dose was chosen in favour of air Kerma or DAP to compare the radiation dose of each imaging technique. Effective dose is a weighted estimate of absorbed tissue and organ radiation and is recommended as the optimal dose comparison metric by the International Commission on Radiological Protection.[9] Unlike air Kerma and DAP, effective dose can be accurately compared between patients of differing body size, habitus, or organ exposure.

Cumulative effective radiation dose was estimated by Monte Carlo simulations using PCXMC (version 2.0) software (STUK, Helsinki, Finland). Previously validated and published methodology was used and a comprehensive description is found on the STUK website, the Radiation and Nuclear Safety Authority of Finland (http://www.stuk.fi/sateilynhyodyntaminen/ohjelmat/PCXMC/en_GB/pcxmc/). Phantom parameters for the PCXMC software included the representative age, height, and weight. Imaging parameters for the PCXMC software included beam shape and position, source-to-subject and subject-to-receptor distance, camera angle, and air Kerma at the interventional reference point. A table attenuation assessment using a 0.18 cc ionisation chamber (Model # 10x5-0.18; Radcal Corporation, Monrovia, California, United States of America) measured an attenuation of 8.8% at the relevant beam quality with a peak energy of 68 kV. The Monte Carlo estimates incorporate this attenuation correction factor. Weighting factors from the 2007 International Commission on Radiological Protection, Publication 103, were used to estimate the effective doses.[9,10]

Image quality phantoms and quality evaluation protocol

One image quality phantom (CIRS) was used for objective assessment of image quality for both the standard imaging technique and AGT. Imaging was performed on the same Philips Allura XP FD 10/10 (Philips Healthcare) biplane fluoroscopy system with the image quality phantom placed on the centre of the fluoroscopy table. Identical parameters including source-to-image distance,

magnification, and anti-scatter grid placement were used for the standard imaging technique and AGT, as described above. Polymethyl methacrylate blocks of 2 cm thick were placed below the image quality phantom to approximate variable chest wall depths of an average neonate (two blocks, 4 cm), 5-year-old (four blocks, 8 cm), and teenager (eight blocks, 16 cm). Images were independently assessed and scored by three blinded reviewers (K.D.H., G.A.F., and R.C.C.) for image blur and contrast loss, with higher scoring denoting superior image resolution and contrast detection. Representative images of the ATOM dosimetry phantoms were also independently evaluated for subjective image quality by three blinded reviewers (K.D.H., G.A.F., and R.C.C.) on a 1–10 scale with the highest overall quality rating denoted as 10. Imaging quality tests were assessed for inter-rater reliability and consistency using two-level mixed effect modelling to assess the effects of the reviewer on variability of the quality rating value through an intra-class correlation coefficient.

Statistical analysis

All statistical analyses were performed using STATA version 15.1 (StataCorp. LLC., College Station, Texas, United States of America). Comparison of continuous variables was performed using two-tailed paired Student's t-test. Multi-level mixed effect modelling was used to assess intra-class correlation as mentioned above. Statistical significance was set at a p value of less than 0.05.

Results

Radiation dose comparison

Tables 1 and 2 summarise anterior–posterior and lateral projection effective doses, air Kerma, DAP, and beam parameters for the three dosimetry phantoms: the neonate, 5-year-old, and teenager across a range of imaging approaches. Of note, effective doses reported for the neonatal and 5-year-old phantom comparison group (i.e. standard recommended imaging) are with the anti-scatter grid already removed consistent with the current guidelines. For the neonatal and 5-year-old phantom, the AGT increased effective doses by 2–92% depending on the imaging projection and magnification setting. Similarly, for the neonatal and 5-year-old phantom, air Kerma levels increased by 2–84% with the AGT. Conversely, for the teenage phantom, the AGT was consistently superior to the standard imaging approach for both anterior–posterior and lateral projections, with effective dose reductions ranging from 5 to 59% and air Kerma reductions ranging from 3 to 16%. Dose reductions were notably greater for imaging in the lateral projection.

Figure 2 compares the effective dose for the AGT versus standard recommended imaging approaches for the three phantoms. Again, the recommended imaging approaches used lower doses than that of AGT in the younger phantoms, but the AGT was superior in the teenage phantom. Because the 5-year-old phantom, representing a 19-kg child, is close to the 20-kg threshold, where guidelines suggest using an anti-scatter grid, we also performed imaging with the anti-scatter grid in place. In this imaging scenario, the AGT reduced dose in the 5-year-old phantom (Supplemental Table S1).

Image quality comparison

Figure 3 demonstrates image quality assessments for the AGT versus standard imaging, and Table 3 summarises objective imaging results. There was no evident difference in objective or subjective

Table 1. Radiation exposure and beam parameters in the anterior–posterior projection with optimised settings

| Phantom | Imaging | Standard imaging | | | | | | Air gap technique | | | | | | % Change in effective dose |
| | | Anterior–posterior projection | | | | | | | | | | | | |
		Mag	KvP	mA (per ms)	Kerma (mGy/1000 frames)	DAP	Effective Dose, mSv/1000 frames (% Error)	Mag	KvP	mA (per ms)	Kerma (mGy/1000 frames)	DAP	Effective dose mSv/1000 frames (% Error)	
Neonate	Cine	6"	67	33.7/ms	4.12	176.5	0.53 (4.9)	8"	68	37.0/ms	5.16	203.1	0.83 (6.1)	↑ 57
		8"	65	29.3/ms	3.15	123.3	0.40 (5.1)	10"	65	30.0/ms	3.40	126.6	0.53 (6.3)	↑ 33
	Fluoro	6"	63	2	1.01	43.5	0.13 (5.0)	8"	65	2	1.30	58.0	0.21 (6.3)	↑ 62
		8"	62	2	0.68	30.3	0.09 (6.8)	10"	62	2	0.74	35.6	0.10 (6.8)	↑ 11
5-year-old	Cine	8"	65	77.0/ms	24.90	1658.0	2.14 (2.2)	10"	63	61.3/ms	28.03	1770.0	2.18 (2.4)	↑ 2
		10"	63	66.3/ms	20.90	1379.6	1.65 (2.2)							↑ 32
	Fluoro	8"	69	3	2.49	191.0	0.24 (2.1)	10"	69	3	2.64	221.0	0.25 (2.3)	↑ 4
		10"	65	2	1.43	127.0	0.13 (2.1)							↑ 92
Teenager	Cine	10"	68	93.2/ms	81.30	8685.0	4.08 (0.7)	10"	67	84.4/ms	68.30	5870.0	3.24 (0.7)	↓ 21
	Fluoro	10"	76	5	6.19	825.0	0.37 (0.7)	10"	77	5	6.00	600.0	0.35 (0.7)	↓ 5

DAP = dose area product; KvP = kilovolt peak; mA = milliamperes; mGy = milliGray; ms= millisecond; mSv = milliSieverts.
All images acquired at 15 frames per second. Copper filtration constant at 0.4 mm copper/1.0 mm aluminium.

Table 2. Radiation exposure and beam parameters in the lateral projection with optimised settings

Phantom	Imaging	Lateral projection												% Change in effective dose
		Standard imaging						Air gap technique						
		Mag	KvP	mA (per ms)	Kerma (mGy/1000 frames)	DAP	Effective dose, mSv/1000 frames (% Error)	Mag	KvP	mA (per ms)	Kerma (mGy/1000 frames)	DAP	Effective dose, mSv/1000 frames (% Error)	
Neonate	Cine	6"	67	35.2/ms	4.63	149.3	0.40 (2.5)	8"	69	39.5/ms	5.97	164.2	0.54 (3.3)	↑35
		8"	66	31.7/ms	3.73	119.4	0.32 (2.5)	10"	68	35.7/ms	4.76	142.9	0.43 (3.3)	↑34
	Fluoro	6"	64	2	1.23	30.8	0.10 (2.5)	8"	65	2	1.54	46.2	0.13 (3.4)	↑30
		8"	63	2	0.90	29.9	0.07 (2.6)	10"	64	2	1.19	44.8	0.10 (3.4)	↑43
5-year-old	Cine	8"	61	40.5/ms	15.30	810.0	1.29 (4.7)	10"	61	40.25/ms	15.60	1020.0	1.31 (4.3)	↑2
		10"	61	42.7/ms	11.30	746.6	0.83 (4.8)							↑58
	Fluoro	8"	67	3	1.90	118.0	0.18 (4.4)	10"	67	3	1.90	114.0	0.18 (4.4)	↑6
		10"	65	2	1.40	77.0	0.12 (4.5)							↑58
Teenager	Cine	10"	68	100/ms	90.10	8829.0	3.09 (0.7)	10"	68	33.8/ms	80.60	5993.0	1.97 (0.8)	↓36
	Fluoro	10"	76	5	6.47	705.0	0.27 (0.7)	10"	75	5	5.78	469.0	0.17 (0.8)	↓59

DAP = dose area product; KvP = kilovolt peak; mA = milliamperes; mGy = milliGray; ms = millisecond; mSv = milliSieverts.
All images acquired at 15 frames/second. Copper filtration constant at 0.4 mm copper/1.0 mm aluminium.

imaging scores from the blinded reviewers for any of the recorded images. Mean image blur scores, where a higher number represents improved image quality, were 6.9 ± 0.2 for standard imaging and 6.9 ± 0.3 for AGT (p = 0.93). Mean contrast loss was 5.5 ± 0.2 for standard imaging and 5.7 ± 0.3 for AGT (p = 0.52). The mean subjective score in the anterior–posterior projection was 6.3 ± 0.5 for standard imaging and 6.2 ± 0.4 for AGT (p = 0.80) with mean in the lateral projection 4.4 ± 0.4 for standard imaging and 4.3 ± 0.4 for AGT (p = 0.75). Pooling all reviewer assessments comparing the AGT to standard imaging (n = 72), the two techniques were equivalent for 65% of all assessments (47/72), the AGT was favoured in 17% (12/72) and standard imaging was favoured in 18% (13/72). Even when favoured, the imaging techniques never differed by a quality score > 1. The three reviewers had unanimous agreement on 11 (46%) of the 24 assessments. For all 11 assessments, the reviewers found the two equivalent imaging techniques. There were no assessments with unanimous agreement of superiority for either imaging technique. Intra-class correlation varied between image quality tests (Table 3).

Discussion

This is the first study to evaluate the use of AGT across a range of patient sizes in paediatric cardiac catheterisation. Using tissue simulation anthropomorphic phantoms, we found that the AGT lowers effective radiation doses in larger patients (i.e. teenagers) during fluoroscopy and cineangiography in both anterior–posterior and lateral projections with the greatest effect seen during lateral projections when the X-ray beam traverses a larger volume of tissue. Conversely, we found that AGT increases effective radiation doses in smaller children (<20 kg) when compared to optimised imaging approaches (i.e. with anti-scatter grid removed). We also found that increased geometric magnification with AGT did not result in an appreciable increase in image blur or reduced contrast differentiation. Taken together, these findings support the use of AGT as a tool to reduce radiation exposure in select scenarios during paediatric cardiac catheterisation. However, it is imperative that providers understand the technique and scenarios where it may be beneficial versus harmful.

Cardiac catheterisation remains a vital diagnostic and interventional tool used in the treatment of children with CHD and acquired heart disease. However, cardiac catheterisation represents the largest source of cumulative radiation exposure in children with heart disease[11] and can sometimes contribute to relatively large cumulative lifetime radiation exposures.[1] Given the association of cumulative radiation exposure to cancer risk, there has been a push to reduce radiation exposure in the catheterisation lab to "as low as reasonably achievable" through the study of novel imaging techniques, education in position statements from national organisations, and quality improvement benchmarks from national databases.[3,11–15]

AGT is a radiation reduction imaging technique originally described in adults undergoing coronary artery imaging.[4] Although AGT has been studied in the paediatric population, previous studies have evaluated this technique in conjunction with other radiation reducing interventions and/or have not evaluated differential effects in larger versus smaller children. Gould et al found up to a 20% mean dose reduction in children undergoing catheterisation with a 15-cm air gap when compared to standard imaging with an anti-scatter grid in place. Importantly, they also demonstrated a reduced number of double-stranded DNA breaks with AGT when compared to standard imaging, providing a
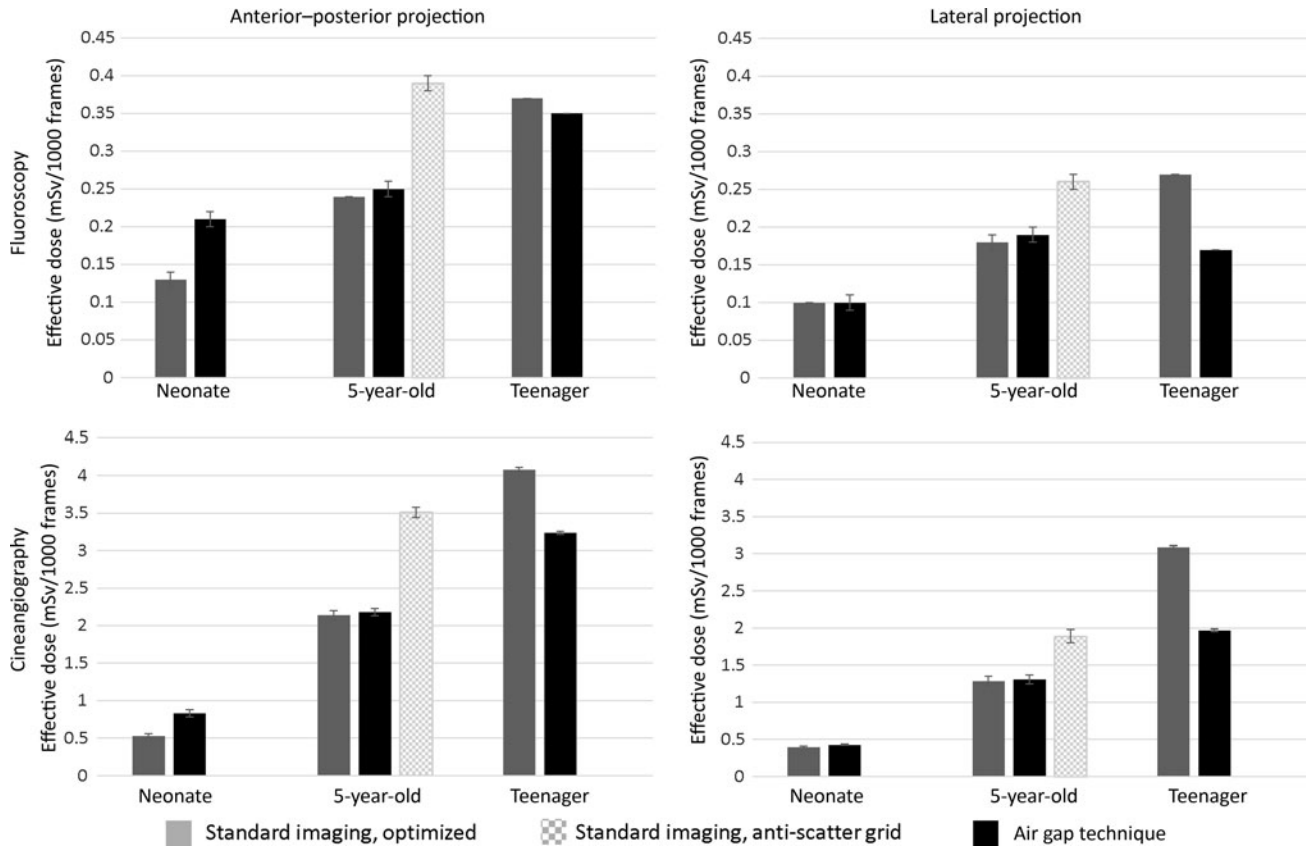
Figure 2. Effect of imaging technique on radiation exposure per imaging projection and representative phantom size (dose estimates represent mSv ± error%). Imaging magnification for neonate, 5-year-old, and teenager: 6, 8, and 10 inches (standard) and 8, 10, and 10 inches (air gap technique, AGT).
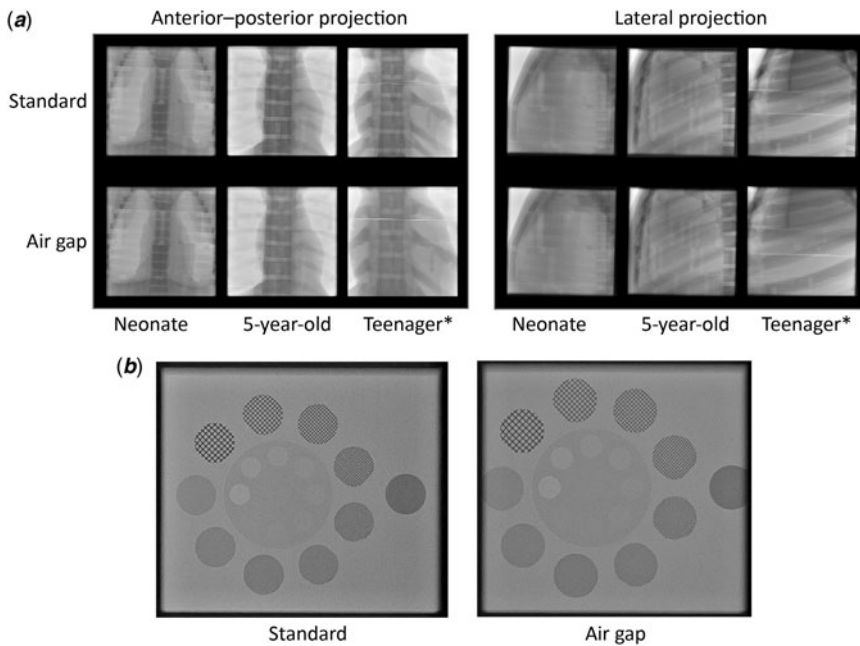

Figure 3. Visual comparison of imaging techniques with CIRS ATOM (*a*) and CIRS QA (*b*) phantoms. *Geometric magnification noted in teenager phantom.

powerful adjunctive measure of the clinical benefit of this dose optimisation approach. However, their results were not stratified by patient size and their baseline comparison involved the use of an anti-scatter grid in all patients including those <20 kg.[16] Our study demonstrated similar dose reductions when comparing AGT to standard imaging with an anti-scatter grid in place

Table 3. Imaging quality assessment results

Phantom	Imaging	Objective image blur ICC: 0.90		Objective contrast loss ICC: 0.43	
		Standard	AGT	Standard	AGT
Neonate	Fluoro	7.7	7.7	5.7	5.7
	Cine	8.0	8.0	5.7	6.3
5-year-old	Fluoro	7.0	7.0	4.7	5.3
	Cine	7.0	7.0	6.3	6.7
Teenager	Fluoro	5.7*	6.0	4.3*	4.3
	Cine	6.0*	6.0	5.7*	5.7

AGT = air gap technique; ICC = intra-class correlation coefficient.
Objective image blur and contrast loss performed on CIRS QA imaging phantom, scale ranging from 1 to 9, with higher score indicating reduced image blur and improved contrast differentiation.
*Anti-scatter grid in place.

(Supplemental Table S1); however, with the anti-scatter grid removed per current recommendations for patients <20 kg,[3] AGT did not provide a dose-reducing benefit. Similarly, Osei et al studied radiation exposure after implementing AGT with other "as low as reasonably achievable" optimisations and found the median total air Kerma and DAP were substantially lower than prior published data for diagnostic or interventional catheterisations in children and infants.[7] However, similar to Gould et al, their "historical" imaging approach included the use of an anti-scatter grid. Our study found that without adjusting any other dose optimising parameters, the AGT was sufficient to lower radiation doses in larger patients, but in smaller patients, where removal of the anti-scatter grid is already recommended,[3] the addition of an air gap alone (i.e. only raising camera height and reducing magnification) actually resulted in higher delivered doses.

With the removal of the anti-scatter grid and introduction of geometric magnification, it is possible that the AGT may impact image quality. In particular, image blur is a concern with excess geometric magnification. Partridge et al. used blinded reviewers and found no significant difference in angiographic image quality; though the average score for the AGT tended to be worse than that with an anti-scatter grid in place.[4] In the paediatric population, Ubeda et al determined that removal of the anti-scatter grid in children without an air gap significantly increased the signal to noise ratio but concluded that the degree of affect did not outweigh the radiation reduction advantage for patients <20 kg.[8] In theory, the use of an air gap in their study would have improved the signal to noise ratio by reducing scatter irradiation, but this was not tested. The current study demonstrated no significant difference in the subjective or objective image quality of AGT compared to standard imaging protocols. Geometric magnification, however, was more evident in the larger dosimetry phantoms.

Taken together, our findings demonstrate that AGT can be a useful dose optimisation strategy with the greatest potential benefit in larger patients, patients where a natural camera offset is required (e.g. to accommodate raised arm positioning), and cases where increased magnification settings are anticipated (e.g. those with a limited area of focus such as coronary angiography). In cases where a broader area of focus is anticipated (e.g. bilateral pulmonary artery angiography), or when the anti-scatter grid is not in use, AGT is less useful and can even increase doses. Figure 4 illustrates a clinical example in which AGT provides a practical advantage to standard imaging. In this case, the patient's arms are positioned over

Figure 4. Clinical scenario illustrating advantage of the AGT in a larger child. Anterior–posterior (AP) source-to-image distance of 113 cm accommodates patient arms in the raised position (arrow). *Anti-scatter grid removed.

the head to prevent brachial plexus injury. Unfortunately, the arm positioning prevents the camera from being maximally lowered, and this will cause auto-exposure controls to increase the dose delivered. Removing the anti-scatter grid (i.e. using AGT) can counteract this effect and will not adversely affect image quality since the "air gap" can serve to filter scatter irradiation from the image receptor.

There are several notable limitations of the current study. All imaging and measurements were performed at a single centre on dosimetry phantoms in controlled settings and not in catheterisation cases with actual patients. Our "standard" imaging approach represents maximally optimised imaging with the camera lowered as far as possible. In clinical settings, the camera is often raised from the maximally lowered position and this will increase delivered dose; therefore, we may have underestimated the benefits of AGT. An advantage of our phantom approach is that it allows for minimisation of confounding variables by controlling test conditions. The results reported were obtained on an older Phillips fluoroscopy system, while newer systems demonstrate significantly reduced radiation.[13] One would expect similar relative reduction trends in newer systems, given that the underlying mechanisms of radiation reduction would be the same regardless of the system used. We also made no attempt to manipulate beam parameters to optimise imaging specifically for AGT, instead relying on the system's automatic exposure control to adjust the imaging parameters. We recognise that it may be possible to further optimise imaging by manipulating the imaging parameters, but we felt this would not reflect a clinically practical approach. Lastly, despite blinding, our image quality assessments are inherently subjective.

Conclusion

When adhering to current imaging recommendations during cardiac catheterisation, AGT should be considered as an effective technique for radiation dose reduction in larger patients where scatter irradiation is significantly increased, particularly in cases when higher magnification is beneficial. In patients <20 kg, the anti-scatter grid should be removed without increasing the source-to-image distance.

References

1. Fazel R, Krumholz HM, Wang Y, et al. Exposure to low-dose ionizing radiation from medical imaging procedures. N Engl J Med 2009; 361: 849–857.
2. Hall J, Jeggo PA, West C, et al. Ionizing radiation biomarkers in epidemiological studies – an update. Mutat Res 2017; 771: 59–84.
3. Hill KD, Frush DP, Han BK, et al. Radiation Safety in children with congenital and acquired heart disease: a scientific position statement on multimodality dose optimization from the image gently alliance. JACC Cardiovasc Imaging 2017; 10: 797–818.
4. Partridge J, McGahan G, Causton S, et al. Radiation dose reduction without compromise of image quality in cardiac angiography and intervention with the use of a flat panel detector without an antiscatter grid. Heart 2006; 92: 507–510.
5. Karoll MP, Mintzer RA, Lin PJ, et al. Air gap technique for digital subtraction angiography of the extracranial carotid arteries. Invest Radiol 1985; 20: 742–745.
6. Roy JR, Sun P, Ison G, et al. Selective anti-scatter grid removal during coronary angiography and PCI: a simple and safe technique for radiation reduction. Int J Cardiovasc Imaging 2017; 33: 771–778.
7. Osei FA, Hayman J, Sutton NJ, Pass RH. Radiation dosage during pediatric diagnostic or interventional cardiac catheterizations using the "air gap technique" and an aggressive "as low as reasonably achievable" radiation reduction protocol in patients weighing <20 kg. Ann Pediatr Cardiol 2016; 9:16–21.
8. Ubeda C, Vano E, Gonzalez L, Miranda P. Influence of the antiscatter grid on dose and image quality in pediatric interventional cardiology X-ray systems. Catheter Cardiovasc Interv 2013; 82: 51–57.
9. The 2007 Recommendations of the International Commission on Radiological Protection. ICRP publication 103. Ann ICRP 2007; 37: 1–332.
10. Rassow J, Schmaltz AA, Hentrich F, Streffer C. Effective doses to patients from paediatric cardiac catheterization. Br J Radiol 2000; 73: 172–183.
11. Johnson JN, Hornik CP, Li JS, et al. Cumulative radiation exposure and cancer risk estimation in children with heart disease. Circulation 2014; 130: 161–167.
12. Hill KD, Wang C, Einstein AJ, et al. Impact of imaging approach on radiation dose and associated cancer risk in children undergoing cardiac catheterization. Catheter Cardiovasc Interv 2017; 89: 888–897.
13. Haas NA, Happel CM, Mauti M, et al. Substantial radiation reduction in pediatric and adult congenital heart disease interventions with a novel X-ray imaging technology. Int J Cardiol Heart Vasc 2015; 6: 101–109.
14. Cevallos PC, Armstrong AK, Glatz AC, et al. Radiation dose benchmarks in pediatric cardiac catheterization: A prospective multi-center C3PO-QI study. Catheter Cardiovasc Interv 2017; 90: 269–280.
15. Ghelani SJ, Glatz AC, David S, et al. Radiation dose benchmarks during cardiac catheterization for congenital heart disease in the United States. JACC Cardiovasc Interv 2014; 7: 1060–1069.
16. Gould R, McFadden SL, Sands AJ, et al. Removal of scatter radiation in paediatric cardiac catheterisation: a randomised controlled clinical trial. J Radiol Prot 2017; 37: 742–760.